Available online at www.sciencedirect.com
SCIENCE DIRECT
Biochemical and Biophysical Research Communications 347 (2006) 363–368
BBRC
www.elsevier.com/locate/ybbrc

The plasma membrane shuttling of CAPRI is related to regulation of mast cell activation

Rika Nakamura [a], Tadahide Furuno [a,b], Mamoru Nakanishi [a,b,*]

[a] Graduate School of Pharmaceutical Sciences, Nagoya City University, 3-1 Tanabe-dori, Mizuho-ku, Nagoya 467-8603, Japan
[b] School of Pharmacy, Aichi Gakuin University, 1-100 Kusumoto-cho, Chikusa-ku, Nagoya 464-8650, Japan

Received 16 June 2006
Available online 23 June 2006

Abstract

The Ca^{2+}-promoted Ras inactivator (CAPRI), a Ras GTPase-activating protein, is involved in the inactivation of mitogen-activated protein kinase pathway. However, a precise role of CAPRI in immune responses is still unknown. Here we showed that overexpression of CAPRI suppresses antigen-induced degranulation and cytokine production in mast cells (RBL cells). Antigen elicited the translocation of CAPRI to the plasma membrane from the cytoplasm, which was concomitant with the increase in the intracellular Ca^{2+} concentration. The nuclear import of extracellular signal-regulated kinase 2 (ERK2) occurred after the re-localization of CAPRI to the cytoplasm in the mast cells, suggesting that the early phase of ERK2 activation is eliminated. A mutant of GAP-related domain, CAPRI(R472S), showed a feeble translocation to the plasma membrane but did not affect the degranulation, ERK2 activation, and cytokine production. The results suggested that the translocation of CAPRI to the plasma membranes regulates crucially cellular responses in mast cells.

Keywords: CAPRI; Calcium ion; Degranulation; MAP kinase; TNF-α; Mast cell

Mast cells express the high-affinity IgE receptors (FcεRI) on their surface, and the aggregation of FcεRI triggers cellular activation. Antigen-induced crosslinking of FcεRI induces the activation of several protein tyrosine kinases including Lyn, Fyn, Syk, and Btk [1]. These events lead to the phosphorylation of linker for activation of T cells (LAT), and the phosphorylated LAT recruits phospholipase C (PLC)γ and adaptor molecules such as Grb2, Grb2-like adaptor downstream of Shc (Gads), and SH2-containing leukocyte protein of 76 kDa (SLP-76) [2]. The phosphorylation of recruited PLCγ produces inositol 1,4,5-triphosphate and diacylglycerol, which elicit the increase in the intracellular Ca^{2+} concentration ($[Ca^{2+}]_i$) and protein kinase C activity. The adaptor protein Grb2 associates a guanine nucleotide exchange factor Sos to convert Ras to its active GTP-bound state. The activated Ras leads to the activation of Raf-1, MEK, and ERK2 which regulates the activity of several transcriptional factors important for cytokine production [3].

Ca^{2+}-promoted Ras inactivator (CAPRI) was identified as a member of the GTPase-activating protein (GAP) 1 family of Ras-specific GAPs [4]. It has two tandem C2 domains which bind Ca^{2+}, a GAP-related domain (GRD), and a pleckstrin homology (PH) domain adjacent to a Btk motif as like other GAP1 family proteins. CAPRI localizes to the cytoplasm in resting cells and translocates to the plasma membrane after the increase in the $[Ca^{2+}]_i$ [4,5]. The C2 domains are essential for the translocation, and the GRD and the PH domain are required for the remaining translocation [5]. The translocation of CAPRI to the plasma membrane was found to lead to the deactivation of Ras and the inhibition of ERKs activation. In addition, macrophages from CAPRI-deficient mice showed a substantial increase in the phosphorylation of ERKs after IgG receptor (FcγR) stimulation [6].

From these results it was considered that CAPRI suppressed receptor-mediated ERK activation through the

* Corresponding author. Fax: +81 52 757 6772.
E-mail address: mamoru@dpc.agu.ac.jp (M. Nakanishi).

0006-291X/$ - see front matter © 2006 Elsevier Inc. All rights reserved.
doi:10.1016/j.bbrc.2006.06.102

deactivation of Ras by the translocation to the plasma membrane after increase in the $[Ca^{2+}]_i$. CAPRI is considered to express ubiquitously in multiple tissue and is also shown to function as an adaptor for Rac and Cdc42 during FcγR-mediated phagocytosis in macrophage [4,6]. However, the effect of CAPRI on the function of immune cells after the ligation of antigen receptors remains unclear. Here we showed that overexpression of CAPRI significantly suppressed FcεRI-mediated degranulation and cytokine production in rat basophilic leukemia (RBL-2H3) cells.

Materials and methods

Materials. A cyan fluorescent protein (CFP) expression vector (pECFP-C1) was purchased from Clontech Laboratories (Palo Alto, CA). A23187 and phorbol myristate acetate (PMA) were obtained from Wako Pure Chemicals (Tokyo, Japan) and Sigma (St. Louis, MO, USA), respectively. Fura 2-AM, Fura Red-AM and BAPTA-AM were from Dojindo (Kumamoto, Japan). Mouse anti-DNP monoclonal IgE (IgE-53-569), DNP-conjugated BSA (DNP-BSA), and yellow fluorescent protein-tagged extracellular signal-regulated kinase 2 (YFP-ERK2) were prepared as described in our previous paper [7]. In our present experiments, seven DNP groups, on the average, were conjugated with BSA.

Plasmids construction. To obtain CAPRI cDNA, poly(A)$^+$ RNA was prepared with a Quickprep Micro mRNA Purification Kit (Amersham Biosciences, Little Chalfont, Buckinghamshire, UK) from NIH-3T3 cells (1×10^7 cells) and served as templates for cDNA synthesis with SuperScript II RT (Gibco-BRL). The DNA sequences coding CAPRI (GenBank Accession No. BC057460) was obtained by RT-PCR with appropriate primer pairs, 5′-*CTCGAG*CAATGGCCAAGCGCAGTTCG-3′ (sense; *Xho*I site is italicized)/5′-*GTCGAG*TCACGTCTGTAGCTCTAGAAGG TGATGGG-3′ (antisense; *Bam*HI site is italicized) using a *Taq* polymerase EX-*Taq* (Takara, Tokyo, Japan). The PCR products were subcloned into a TA cloning vector pCRII (Invitrogen) and sequenced with an Applied Biosystems 3130xl genetic analyzer to verify the DNA sequence of CAPRI. The full-length cDNA coding CAPRI was ligated with pECFP-C1 expression vectors at *Xho*I and *Bam*HI sites. The cDNA for a GRD mutant of CAPRI (CAPRI(R472S)) in which Arg^{472} is substituted with Ser was prepared by the overlap extension method using a primer pair containing mutated region (5′-CATTCATCGAGCTCACCAGCTTCCT-3′ and 5′-AGGAAGCTGGTGAGCTCGATGAATG-3′). The DNA coding CAPRI(R472S) was also ligated with pCRII, and its sequence was confirmed by DNA sequencing.

Cell culture and transfection. RBL-2H3 cells were cultured in an atmosphere of 5% CO_2 at 37 °C in MEM (Nissui, Tokyo, Japan) supplemented with 10% fetal calf serum (FCS) (Boehringer Mannheim, Indianapolis, IN, USA). The cells were electroporated in cold K^+-PBS with 40 μg of plasmid DNA at 250 V and 950 μF using Gene Pulser (Bio-Rad, Richmond, CA). RBL-2H3 cells transfected with plasmid DNAs were maintained in culture dishes for a few days and were used for the experiments. The stable transfectant cells were obtained by the selection with antibiotic G418 (Sigma).

Microscopic measurements. The RBL-2H3 cells were harvested from culture dishes and transferred to an observation chamber (Elecon, Chiba, Japan). After incubating overnight, the cells were treated with mouse anti-DNP IgE, Fura Red-AM (1 μM), or BAPTA-AM (5 μM) for 20 min, if necessary. Then the cells were washed with Hepes buffer (10 mM Hepes (pH 7.2), 140 mM NaCl, 5 mM KCl, 0.6 mM $MgCl_2$, 1 mM $CaCl_2$, 0.1% glucose, 0.1% BSA, and 0.01% sulfinpyrazone). The preparations were viewed in a confocal laser scanning microscope (CLSM) (LSM-510; Zeiss, Oberkochen, Germany). CFP was excited with an argon ion laser (458 nm) and its fluorescence was detected by a long path filter (>515 nm). To detect CFP and Fura Red fluorescence simultaneously, CFP and Fura Red were excited at 458 nm and at 488 nm, and their fluorescence was observed by a band path filter (475–525 nm) and a long path filter (>560 nm), respectively. To detect CFP and YFP fluorescence simultaneously, CFP and YFP were excited at 458 nm and 488 nm, and their fluorescence was observed by a band path filter (475–525 nm) and a long path filter (>530 nm), respectively [7]. The temperature of the observation chambers was maintained at 37 °C during experiments.

Data analysis. For analysis for translocation to the plasma membrane of CAPRI, the fluorescence intensities of CFP-CAPRI or CFP-CAPRI(R472S) in a region of interest in the cytoplasm were measured in a series of images. After background fluorescence was subtracted from the image series, the ratio of the fluorescence intensity at each time point (F_t) and that at the first image before the addition of stimulants at the same area (F_0) was calculated. The translocation (%) was estimated by the equation; $(1 - F_t/F_0) \times 100$. For analysis for translocation to the nucleus of ERK2, the fluorescence intensity of YFP-ERK2 in a region of interest in the nucleus was measured in a series of images. After background fluorescence was subtracted from the image series, the ratio of the fluorescence intensity at each time point (F_t) and that at the first image before the addition of stimulants at the same area (F_0) was calculated. The translocation (%) was estimated by the equation; $(F_t/F_0 - 1) \times 100$. For analysis of $[Ca^{2+}]_i$ movements, the fluorescence intensities of Fura Red was measured in a series of images. After background fluorescence was subtracted from the image series, the ratio of the fluorescence intensity at each time point (F_t) and that at the first image before the addition of stimulants at the same area (F_0) was calculated. The fluorescence intensity change of Fura Red (%) was shown by the equation; $(F_t/F_0 - 1) \times 100$.

$[Ca^{2+}]_i$ measurement. RBL-2H3 cells (1×10^6 cells) were loaded with Fura 2-AM (1 μM) and anti-DNP IgE (0.2 μg/ml) for 20 min, and washed twice with Hepes buffer. The fluorescence intensity was measured with an excitation wavelength of 340 nm or 360 nm and an emission wavelength of 500 nm by a spectrofluorometer (RF-5300PC, Shimadzu, Kyoto, Japan) at 37 °C. The ratio values (F_{340}/F_{360}) were converted to the $[Ca^{2+}]_i$ by the procedure reported previously [9].

β-Hexosaminidase secretion. Degranulation of RBL cells was monitored by measuring the activity of a granule-stored enzyme, β-hexosaminidase, secreted in the RBL cell supernatants. Briefly the cells were plated in 24-well plates at 5×10^4 cells/well. On the following day, the cells were sensitized by anti-DNP IgE (0.2 μg/ml) for 30 min, then monolayers were washed in Hepes buffer and incubated with DNP-BSA or A23187 plus PMA at 37 °C. Following the incubation, aliquots of the supernatants were transferred to 96-well plates (20 μl/well) and incubated with 20 μl of a substrate solution (2 mM *p*-nitrophenyl-*N*-acetyl-β-D-glucosaminide (Sigma) in 0.1 M citrate, pH 4.5) for 1 h at 37 °C. After terminating of the reaction with 160 μl of 0.167 M Na_2CO_3–$NaHCO_3$ buffer, the absorbance at 405 nm was measured by a microplate reader (MRR-A4, TOSOH, Japan). The release activity relatively to the total β-hexosaminidase content of the cells was calculated. The total β-hexosaminidase content was determined by dissolving cells with 0.1% Triton X-100 [9]. Each assay was performed in triplicate. Results were tested statistically by unpaired two-tailed Student's *t*-test and were considered statistically significant when $P < 0.01$.

Western blot. Western blotting analysis was performed by the previous procedures [7,8]. To prepare whole cell lysate, collected RBL cells were suspended in lysis buffer (20 mM Hepes, pH 7.3, 1% Triton X-100, 1 mM EDTA, 50 mM NaF, 2.5 mM *p*-nitrophenyl phosphate, 1 mM Na_3VO_4, 10 μg/ml phenylmethylsulfonyl fluoride, 10 μg/ml leupeptin, and 10% glycerol) and allowed to stand on ice for 30 min. The suspension was clarified by centrifugation (150,000*g*, 20 min). After centrifugation, the resulting supernatants were solubilized by treatment with Laemmli buffer at 100 °C for 3 min and separated by electrophoresis in 8% SDS–polyacrylamide gel. The electrophoresed proteins were transferred to PVDF membrane with an electroblotter. After blocking with 0.5% casein, the membranes were probed with rabbit anti-phospho MEK antibody (1:1000 dilution), anti-phospho ERK1/2 antibody (1:1000 dilution), or anti-ERK1/2 antibody (1:2000 dilution) (Cell Signaling Technology, Beverly, MA) and treated with 1:1000 dilution HRP-labelled anti-rabbit IgG (Santa Cruz, CA; 0.4 μg/ml). The amount of HRP-labelled IgG bound to each protein band was determined by LAS-3000 (Fuji Film).

TNF-α production. RBL-2H3 cells (5×10^4 cells/well in 24-well plates) were sensitized by anti-DNP IgE (0.2 μg/ml) for 30 min, then monolayers were washed in Hepes buffer and stimulated with DNP-BSA for 3 h at 37 °C. The supernatant was collected from each well and the absolute amount of TNF-α released from cells was determined using a rat TNF-α immunoassay system (Techne Corporation, Minneapolis, MN, USA) [8]. Experimental results are expressed as mean and SEM. Results were tested statistically by unpaired two-tailed Student's *t*-test and were considered statistically significant when $P < 0.01$.

Results

Translocation of CFP-CAPRI to the plasma membranes

After establishing monoclonal RBL-2H3 cell lines stably expressing CFP-CAPRI and CFP-CAPRI(R472S), we studied their intracellular dynamics by CLSM. CAPRI localized in the cytoplasm and moved to the plasma membranes within 1 min after the addition of antigen (DNP-BSA; 0.2 μg/ml) to RBL cells as shown in Fig. 1a and b. The translocation of CAPRI on the plasma membrane of the cells became the maximum at ~1.5 min, and then they returned to the cytoplasm from the plasma membranes. CAPRI(R472S) translocated to the plasma membranes from the cytoplasm as CAPRI did after the ligation of FcεRI, however, its amount of the translocation was less than that of CAPRI (Fig. 1b). To understand the relationship between the $[Ca^{2+}]_i$ and the translocation of CAPRI, we measured the $[Ca^{2+}]_i$ and the distribution of CAPRI at the same time after antigen stimulation. The translocation of CAPRI occurred invariably after the $[Ca^{2+}]_i$ had increased, as shown in Fig. 1c. CAPRI never moved to the plasma membranes when the $[Ca^{2+}]_i$ did not increase in the mast cells. The pretreatment of the cells with calcium chelator BAPTA-AM inhibited the antigen-induced translocation of CAPRI or CAPRI(R472S) to the plasma membranes (Fig. 1d). On the contrary, the calcium ionophore A23187 (1 μM) induced them to translocate to the plasma membranes as shown in Fig. 1e. The results indicated that CAPRI translocated from the cytoplasm to the plasma membrane after the ligation of FcεRI in the RBL cells and that the plasma membrane shuttling of CAPRI was dependent on the increment of the $[Ca^{2+}]_i$.

Suppression of degranulation by CAPRI

To study the effects of CAPRI on mast cell function, we compared the degranulation among wild type, CFP-CAPRI-expressing, and CFP-CAPRI(R472S)-expressing RBL-2H3 cells. First, we measured the increases of $[Ca^{2+}]_i$ following the addition of antigen. The $[Ca^{2+}]_i$ was

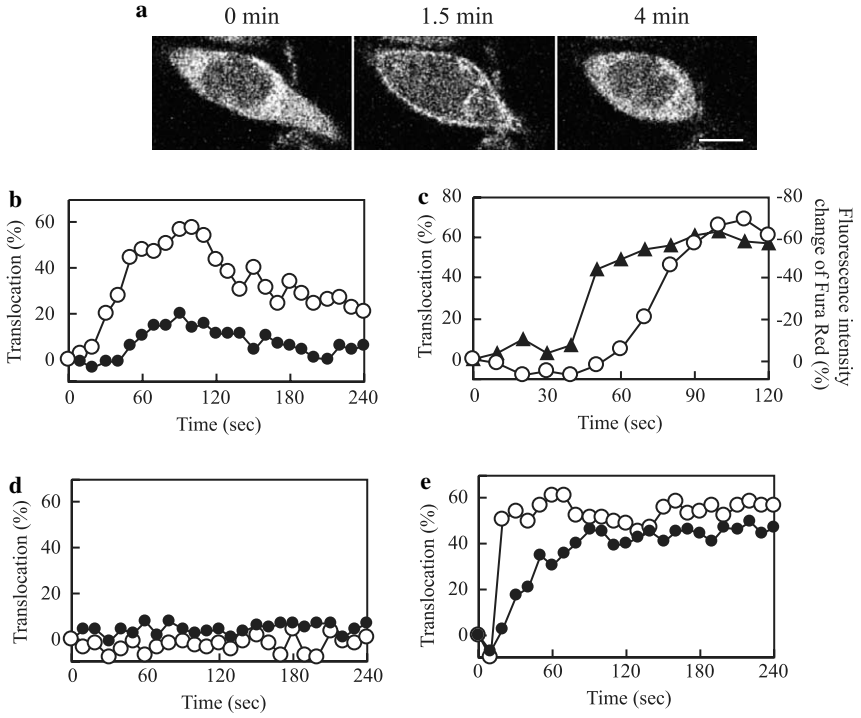

Fig. 1. The Ca^{2+} dependence of the translocation to the plasma membrane of CAPRI. (a) Sequential fluorescence images of CFP-CAPRI in an RBL-2H3 cell after the addition of antigen (DNP-BSA; 0.2 μg/ml). Bar = 10 μm. (b) Time-courses of the translocation to the plasma membrane of CFP-CAPRI (open circles) and CFP-CAPRI(R472S) (closed circles) after antigen stimulation (DNP-BSA; 0.2 μg/ml). (c) Simultaneous measurement of the $[Ca^{2+}]_i$ movement and the CAPRI translocation. Time-courses of the fluorescence intensity change of Fura Red (closed triangles) and translocation to the plasma membrane of CFP-CAPRI (open circles) after antigen stimulation (DNP-BSA; 0.2 μg/ml) in a Fura Red-loaded RBL-2H3 cell expressing CFP-CAPRI. (d) Time-courses of the translocation to the plasma membrane of CFP-CAPRI (open circles) and CFP-CAPRI(R472S) (closed circles) after antigen stimulation (DNP-BSA; 0.2 μg/ml) in RBL-2H3 cells pretreated with BAPTA-AM. (e) Time-courses of the translocation to the plasma membrane of CFP-CAPRI (open circles) and CFP-CAPRI(R472S) (closed circles) after the addition of calcium ionophore (A23187; 1 μM).

~50 nm in resting RBL cells, and then increased at ~150 nm after antigen stimulation in each cell line (see Fig. 2a), showing that there are no significant differences for the antigen-induced $[Ca^{2+}]_i$ increments among three different cell lines. However, the secretion of β-hexosaminidase was quite different among three cell lines. The β-hexosaminidase secretion was greatly inhibited in CFP-CAPRI-expressing cells. But such kinds of suppression was not observed in CFP-CAPRI(R472S)-expressing cells as shown in Fig. 2b. Similar kinds of suppression for the β-hexosaminidase secretion were also observed in CFP-CAPRI-expressing cells when they were stimulated with A23187 and PMA (Fig. 2b). The results showed that the translocation of CAPRI to the plasma membranes plays a key role for suppression of the degranulation in RBL-2H3 cells.

Effects of CAPRI on ERK activation

Next, we studied the effects of CAPRI on FcεRI-mediated ERK activation in RBL cells. As described in our previous paper [7], YFP-ERK2 translocated to the nucleus

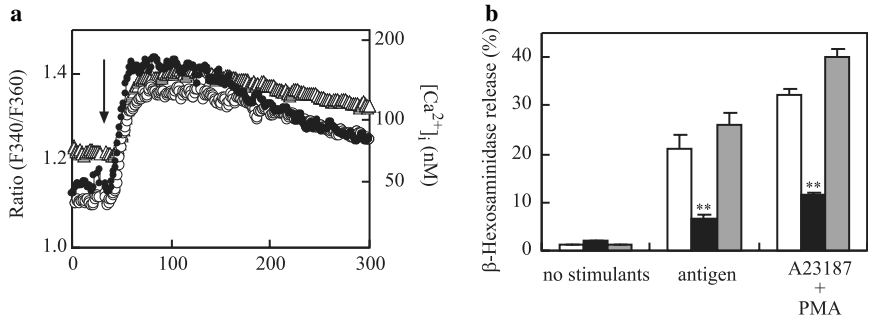

Fig. 2. Suppression of the degranulation by CAPRI in RBL-2H3 cells. (a) The increase of the $[Ca^{2+}]_i$ after the addition of antigen (DNP-BSA; 0.2 μg/ml) in wild type cells (open triangles), CFP-CAPRI-expressing cells (open circles), and CFP-CAPRI(R472S)-expressing cells (closed circles) by a spectrofluorometer. An arrow shows the time when antigen was added. (b) The secretion of β-hexosaminidase from wild type cells (white bars), CFP-CAPRI-expressing cells (black bars), and CFP-CAPRI(R472S)-expressing cells (grey bars). The percentages of released β-hexosaminidase to total contents in cells for 30 min assay without stimulants (left), with antigen (DNP-BSA; 0.2 μg/ml) (middle), and with A23187 (1 μM) and PMA (50 ng/ml) (right). $^{**}P < 0.01$ compared with wild type cells.

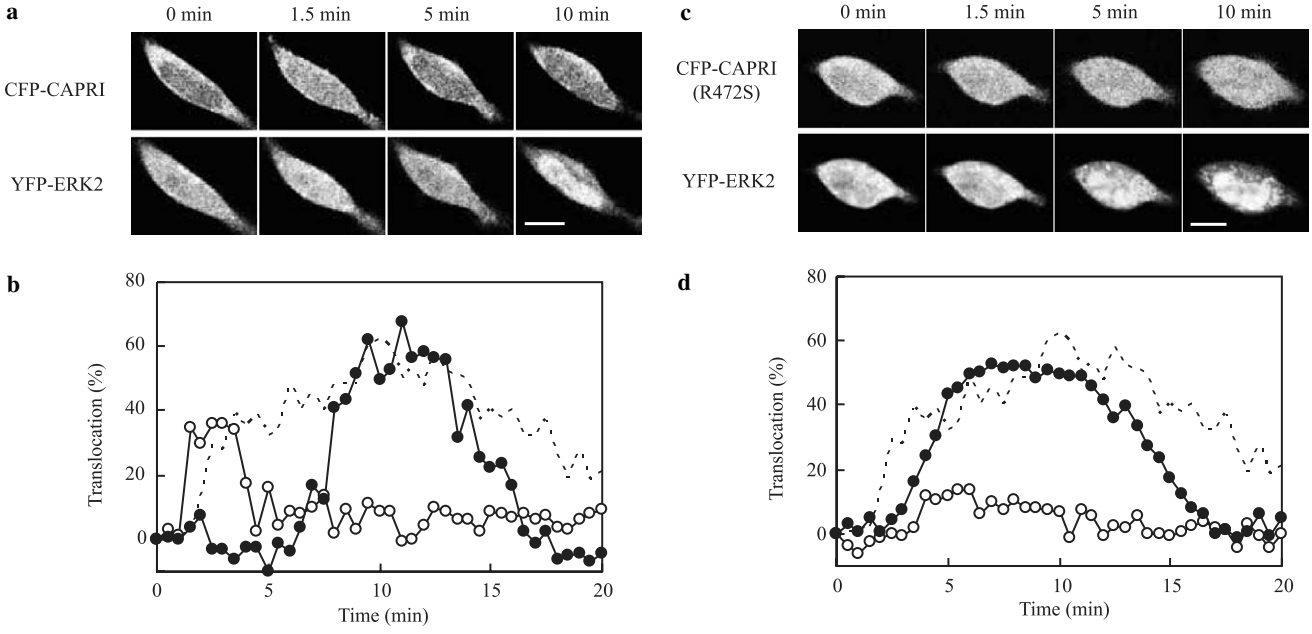

Fig. 3. Effect of CAPRI on intracellular movement of ERK2 in RBL-2H3 cells. (a) Sequential fluorescence images of CFP-CAPRI and YFP-ERK2 in an RBL-2H3 cell after the addition of antigen (DNP-BSA; 0.2 μg/ml). Bar = 10 μm. (b) Time-courses of the translocation from the cytoplasm to the plasma membrane of CFP-CAPRI (open circles) and the translocation from the cytoplasm to the nucleus of YFP-ERK2 (closed circles) after antigen stimulation (DNP-BSA; 0.2 μg/ml). The representative time-course of nuclear translocation of YFP-ERK2 in wild type RBL-2H3 cells after antigen stimulation (DNP-BSA; 0.2 μg/ml) is shown as a broken line. (c) Sequential fluorescence images of CFP-CAPRI(R472S) and YFP-ERK2 in an RBL-2H3 cell after the addition of antigen (DNP-BSA; 0.2 μg/ml). Bar = 10 μm. (d) Time-courses of the translocation to the plasma membrane of CFP-CAPRI(R472S) (open circles) and the translocation to the nucleus of YFP-ERK2 (closed circles) after antigen stimulation (DNP-BSA; 0.2 μg/ml). The representative time-course of nuclear translocation of YFP-ERK2 in wild type RBL-2H3 cells after antigen stimulation (DNP-BSA; 0.2 μg/ml) is shown as a broken line.

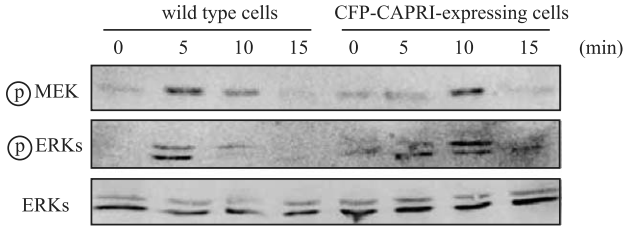

Fig. 4. Western blotting analysis for the FcεRI-induced phosphorylation of MEK and ERKs in wild type RBL-2H3 cells and CFP-CAPRI-expressing RBL-2H3 cells. Western blots of whole cell lysates were carried out by anti-phospho MEK antibody (upper panel), anti-phospho ERK1/2 antibody (middle panel), and anti-ERK1/2 antibody (lower panel).

from the cytoplasm within 4–5 min after the addition of antigen, and thereafter the imported ERK2 was exported from the nucleus at ~15 min in RBL cells as shown in Fig. 3 (broken lines). The time-courses of the nuclear shuttling were consistent with that of phosphorylation of ERK2 [7]. In CFP-CAPRI-expressing cells, however, the translocation of CAPRI to the plasma membrane occurred at first, and ERK2 moved to the nucleus after the return of CAPRI to the cytoplasm from the plasma membrane (~5 min after the addition of antigen), as shown in Fig. 3a and b. The imported ERK2 went back to the cytoplasm within ~15 min after antigen stimulation. The ERKs phosphorylation was actually shown to be inhibited at 5 min after antigen stimulation in CFP-CAPRI-expressing cells by Western blotting, as shown in Fig. 4. The activation of MEK was also suppressed at 5 min after antigen stimulation in CFP-CAPRI-expressing cells. On the other hand, the antigen-induced intracellular movement of ERK2 in CFP-CAPRI(R472S)-expressing cells was not suppressed and was similar to wild type cells, as shown in Fig. 3c and d. These results suggested that CAPRI functioned as Ras GAP when it translocated to the plasma membrane and that it suppressed the early phase of ERK2 activation after the ligation of FcεRI through the inhibition of upstream of MAP kinase cascade.

Inhibition of TNF-α production by CAPRI

To study the effect of inhibition of ERK2 activation in the early phase on transcriptional activity, we compared the FcεRI-induced TNF-α production among wild type, CAPRI-expressing, and CAPRI(R472S)-expressing cells. Produced TNF-α at 3 h after antigen addition was significantly suppressed (48 ± 41 pg/10^6 cells) in CAPRI-expressing cells in comparison with those in wild type (195 ± 24 pg/10^6 cells) and CAPRI(R472S)-expressing cells (144 ± 48 pg/10^6 cells). The results suggested that the inhibition of ERK2 activation in early phase by CAPRI induced the suppression of TNF-α production.

Discussion

The Ras superfamily of small G proteins plays important roles in many types of cells. Ras proteins are known to be binary switches by cycling between inactive GDP-bound and activate GTP-bound forms and regulate multiple cellular signalling pathways [10]. Guanine nucleotide exchanging factors (GEFs) and GAPs are intimately involved in the extent and duration of Ras activation. In mast cells, the protein tyrosine kinase Syk phosphorylates LAT, which then recruit the adaptor molecules Grb2, Gads, and SLP-76. Ras proteins are activated by Grb2-associated effector molecule, Sos, which is a GEF at the plasma membrane. In addition, a mast cell-restricted Ras guanine nucleotide-releasing protein, Ras GRP4, which has recently been identified, is known to contribute differentiation, granule maturation, and prostaglandin D_2 (PGD_2) expression [11,12]. However, the mechanism for the regulation of Ras activation has been unclear yet in mast cells.

Here we have studied the effect of a member of Ras GAP, CAPRI, whose expression was detected at mRNA level in RBL-2H3 cells, on mast cell activation. CAPRI distributed in the cytoplasm in resting state, and translocated to the plasma membrane after the increase in $[Ca^{2+}]_i$ following the ligation of FcεRI. Thereafter the CAPRI localized at the plasma membrane returned to the cytoplasm. The translocation of CAPRI to the plasma membrane was inhibited by the pretreatment of BAPTA-AM (see Fig. 1d) and was induced by the addition of A23187 (see Fig. 1e) or thapsigargin, an inhibitor of sarcoplasmic/endoplasmic-reticulum Ca^{2+}-ATPases (data not shown), indicating that it was also dependent on the $[Ca^{2+}]_i$ increment in RBL-2H3 cells as described in the previous papers using COS, CHO, and HeLa cells [4,5]. The duration of its localization at the plasma membrane was ~5 min and then it returned to the cytoplasm in the case of antigen stimulation. On the other hand, the extent and duration of translocation to the plasma membrane of CAPRI(R472S), which is known to has much less activity as GAP by a point mutation in GRD, have weaker and shorter than those of wild type CAPRI. This suggested that GRD in CAPRI was required for the stable binding to Ras at the plasma membrane.

Such plasma membrane shuttling of CAPRI in initial phase was found to elicit in the suppression of cellular activation. Antigen-induced $[Ca^{2+}]_i$ movement occurred normally in RBL-2H3 cells expressing CFP-CAPRI, but the subsequent cellular response such as degranulation, ERKs activation, and TNF-α production was significantly inhibited. In RBL-2H3 cells expressing CFP-CAPRI(R472S), the suppression of cellular response was not found. These results suggested that overexpression of CAPRI negatively regulated the cellular signaling in downstream of Ca^{2+}. From real-time imaging analysis of CAPRI and ERK2, ERK2 was not shown to translocate to the nucleus while CAPRI localized at the plasma membrane after the addition of antigen in CFP-CAPRI-expressing cells. ERK2 started to move to the nucleus after CAPRI returned to the cytoplasm, but this delayed nuclear import of ERK2 did not induce the promotion of TNF-α. The translocation to the plasma membrane of CAPRI inhibited FcεRI-mediated MEK phosphorylation in the early phase as well as

ERKs phoshorylation, indicating that CAPRI negatively controlled the activation of MAP kinase cascade.

This is the first report showing the role of CAPRI in mast cell activation. The demonstration that CAPRI down-regulated cellular function by the temporal translocation to the plasma membrane following the increase in $[Ca^{2+}]_i$ indicates the importance of Ras activation in initial phase of antigen stimulation in cellular response in RBL-2H3 cells. The facts described here must provide valuable information for inflammation and allergic reaction.

References

[1] S.J. Galli, J. Kalesnikoff, M.A. Grimbaldeston, A.M. Piliponsky, C.M.M. Williams, M. Tsai, Mast cells as "tunable" effector and immunoregulatory cells: recent advances, Annu. Rev. Immunol. 23 (2005) 749–786.

[2] J. Rivera, Molecular adapters in FcεRI signaling and the allergic response, Curr. Opin. Immunol. 14 (2002) 688–693.

[3] B. Jabril-Cuenod, C. Zhang, A.M. Scharenberg, R. Paolini, R. Numerof, M.A. Beaven, J.P. Kinet, Syk-dependent phosphorylation of Shc: a potential link between FcεRI and the Ras/mitogen-activated protein kinase signaling pathway through SOS and Grb2, J. Biol. Chem. 271 (1996) 16268–16272.

[4] P.J. Lockyer, S. Kupzig, P.J. Cullen, CAPRI regulates Ca^{2+}-dependent inactivation of the Ras-MAPK pathway, Curr. Biol. 11 (2001) 981–986.

[5] Q. Liu, S.A. Walker, D. Gao, J.A. Taylor, Y.F. Dai, R.S. Arkell, M.D. Bootman, H.L. Roderick, P.J. Cullen, P.J. Lockyer, CAPRI and RASAL impose different modes of information processing on Ras due to contrasting temporal filtering of Ca^{2+}, J. Cell Biol. 170 (2005) 183–190.

[6] J. Zhang, J. Guo, I. Dzhagalov, Y.W. He, An essential function for the calcium-promoted Ras inactivator in Fcγ receptor-mediated phagocytosis, Nat. Immunol. 6 (2005) 911–919.

[7] T. Furuno, N. Hirashima, S. Onizawa, N. Sagiya, M. Nakanishi, Nuclear shuttling of mitogen-activated protein (MAP) kinase (extracellular signal-regulated kinase (ERK) 2) was dynamically controlled by MAP/ERK kinase after antigen stimulation in RBL-2H3 cells, J. Immunol. 166 (2001) 4416–4421.

[8] N. Ohyama, T. Furuno, N. Hirashima, M. Nakanishi, The effects of ITIM-bearing FcγRIIB on the nuclear shuttling of MAP kinase in RBL-2H3 cells, Immunol. Lett. 90 (2003) 173–176.

[9] N. Kato, M. Nakanishi, N. Hirashima, Cholesterol depletion inhibits store-operated calcium currents and exocytotic membrane fusion in RBL-2H3 cells, Biochemistry 42 (2003) 11808–11814.

[10] S.A. Walker, P.J. Lockyer, P.J. Cullen, The Ras binary switch: an ideal processor for decoding complex Ca^{2+} signals? Biochem. Soc. Trans. 31 (2003) 966–969.

[11] Y. Yang, L. Li, G.W. Wong, S.A. Krilis, M.S. Madhusudhan, A. Šali, R.L. Stevens, RasGRP4, a new mast cell-restricted Ras guanine nucleotide-releasing protein with calcium- and diacylglycerol-binding motifs: identification of defective variants of this signaling protein in asthma, mastocytosis, and mast cell leukemia patients and demonstration of the importance of RasGRP4 in mast cell development and function, J. Biol. Chem. 277 (2002) 25756–25774.

[12] L. Li, Y. Yang, R.L. Stevens, RasGRP4 regulates the expression of prostaglandin D2 in human and rat mast cell line, J. Biol. Chem. 278 (2003) 4725–4729.